AN EXPERIMENTAL INVESTIGATION OF THE STABILITY OF SHELLS IN CREEP

A. P. Kuznetsov and N. M. Yungerman

Zhurnal Prikladnoi Mekhaniki i Tekhnicheskoi Fiziki, No. 4, pp. 128-131, 1965

Below we present the results of an experimental investigation into the creep stability of thin-walled cylindrical Duralumin shells in compression and pure bending.

The stability tests in bending and the tests on one batch of specimens in compression were carried out on special lever-type testing machines on which various types of constant load could be applied to heated specimens: axial force, bending moment, torque, etc. On these machines the constant load is maintained by means of a suspended weight. The testing of another batch of specimens in compression was carried out on a TsDM-30 hydraulic testing machine with a single-section furnace. In this case the constant load was maintained by an automatic device connected to the hydraulic system of the machine. The accuracy with which the load was maintained was in all cases ±2%.

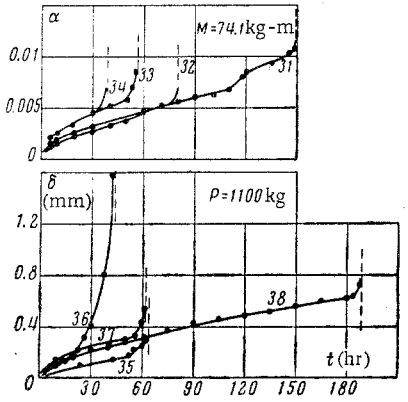

Fig. 1

On the lever-type machines the specimens were heated in electric furnaces with five individual heating sections. Independent control of the stress across each section produced a sufficiently uniform temperature field in the specimen. For example, in bending tests the spread of temperature over the working length of the specimen did not exceed ±2 deg C, while in the compression tests it was ±5 deg C. During the tests a constant temperature was maintained with an accuracy of ±2 deg C by means of a EPD-12 potentiometer, while the temperature field was measured with a EPP-09 recording device. Chromel-alumel thermocouples were used to record temperature.

The shell specimens used in these tests were machined from extruded D16T Duralumin tubing. The nominal shell dimensions were as follows: internal diameter d = 175 mm, wall thickness δ = 0.5 mm, length l = 425 mm (working length about 360 mm), and width of end closures 12 mm. Thus, the specimens could be classified as long thin shells.

The specimens were checked by measuring the mutually perpendicular diameters d_1 and d_2 in three different cross sections and the wall thickness. These measurements showed that the deviations from the nominal wall thickness over the working length did not exceed ±0.02 mm, while the relative ovalness $(d_1 - d_2)/d_1$ was 1-2%. Careful measurements showed that the initial irregularities had no definite form and no axial symmetry and could be represented along the generator as long half-waves (with a length equal to the length of the shell) and two to three superposed shorter half-waves of various lengths with amplitudes from 0.1 to 0.6 mm and 0.05-0.15 mm, respectively. Since the initial irregularities of each specimen have their own geometry, it is not possible to compare the specimens with respect to a definite parameter. The initial irregularities are described here only in order to show the quality of machining.

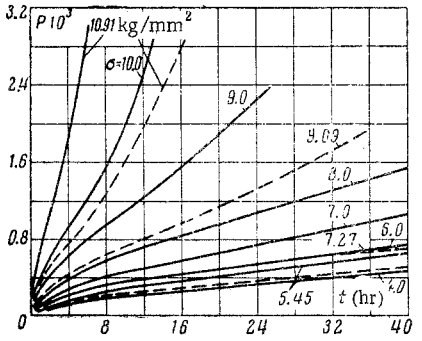

Fig. 2

The specimens were tested at 255 deg C. Each specimen was heated to the required temperature in about 1-2 hr and held at this temperature for about 0.5 hr before the gradual application of the load, which was maintained during the entire test. Loading was continued until the actual moment of failure of the specimen, which took place instantaneously with a "bang." Observation of the surface of the specimens through small windows in the furnaces showed that most of the time, from the moment of load application to the moment of failure, no deformation of the surface was apparent. Shortly before failure a small dent appeared in the surface, and the development of this dent eventually led to abrupt loss of load-carrying ability. In the case of bending the place where the dent appears corresponds to the maximum compressive stress, while in the case of axial compression the dent may appear anywhere.

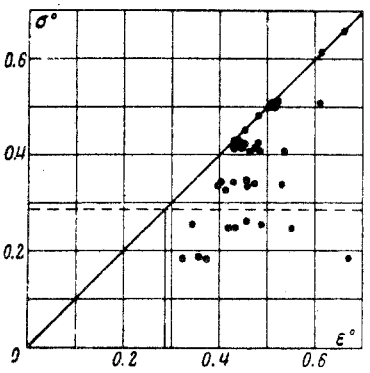

Fig. 3

During the axial compression tests the longitudinal strain was measured by means of dial gauges with 0.01-mm graduations. During the bending tests dial gauges were used to measure the rotation of the end section, the displacement of the end section in the plane of application of the moment, and the flattening of the central portion of the shell. All these deformations were probably due not only to creep of the middle surface but also to bending of the shell surface due to initial irregularities. The graphs of Fig. 1 show the measured displacements under a load P = 1100 kg (axial compression) and a moment

Table 1

№	P, kg	δ,mm	σ, kg/mm²	t*, hr
		First batch		
1	3.640	0.50	13.23	0
2	3.900	0.50	14.17	0
3	2.870	0.48	10.83	0
4	2.850	0.50	10.36	0
5	3.000	0.50	10.90	1.33
6	3.000	0.50	10.90	0.05
7	2.500	0.50	9.08	0.16
8	2.500	0.52	8.73	1.5
9	2.500	0.52	8.73	5.0
10	2.000	0.52	6.97	7.42
11	2.000	0.49	7.41	5.16
12	2.000	0.49	7.41	8.33
13	1.500	0.49	5.55	58.11
14	1.500	0.50	5.45	54.9
15	1.500	0.50	5.45	17.33
		Second batch		
16*	~2.700	0.51	9.62	0
17	~2.500	0.49	9.26	0
18	3.000	0.51	10.67	0.03
19	3.000	0.50	10.90	0
20	3.000	0.51	10.67	0.02
21	2.500	0.52	8.73	0.53
22*	2.500	0.49	9.25	0
23	2.500	0.51	8.90	0.11
24	2.500	0.51	8.90	0.55
25	2.500	0.51	8.90	0.25
26	2.500	0.50	9.08	0.54
27	2.000	0.51	7.16	7.58
28	2.000	0.50	7.27	18.33
29	2.000	0.49	7.41	2.75 (2.33)
30	2.000	0.50	7.27	3.00
31	2.000	0.50	7.27	9.83
32	1.500	0.50	5.45	53.75 (27)
33	1.500	0.50	5.45	34.5
34	1.500	0.51	5.32	71.0 (53) (60.5)
35	1.100	0.51	3.91	65.0
36	1.100	0.51	3.91	43.0
37	1.100	0.50	3.99	62.0 (56)
38	1.100	0.50	3.99	192.28

An asterisk* denotes specimens with large initial irregularities. If the test was interrupted, the figure in parentheses shows the time at which the interruption occurred.

Table 2

№	M, kg·m	δ,mm	σ_{max}, kg/mm²	t*, hr
1	96.4	0.51	7.67	0
2	129.2	0.50	10.48	0
3	135	0.50	10.92	0
4	130.7	0.50	10.60	0
5	90.0	0.51	7.15	0
6	94.0	0.49	7.78	0.5
7	94.0	0.51	7.47	0.03
8	94.0	0.51	7.47	0.07
9	94.0	0.50	7.63	34,91 (15.5)
10	94.0	0.51	7.47	7.59
11	94.0	0.50	7.63	6.17
12	94.0	0.51	7.47	5.08
13	94.0	0.51	7.47	2.59
14	85.9	0.50	6.96	10.75
15	85.9	0.50	6.96	8.40
16	85.9	0.50	6.96	4.25 (3)
17	85.9	0.52	6.70	3.40
18	85.9	0.51	6.82	2.00
19	85.9	0.49	7.11	20.77
20	85.9	0.50	6.96	19.75
21	85.9	0.50	6.96	16.02
22	85.9	0.50	6.96	5.75
23	85.9	0.50	6.96	1.59
24	80.6	0.50	6.54	3.17
25	80.6	0.50	6.54	36.83
26	80.6	0.51	6.40	41.25 (34)
27	80.6	0.52	6.28	24.00
28	80.6	0.51	6.40	22.50 (16)
29	80.6	0.51	6.40	14.03
30	80.6	0.47	6.95	7.25
31	74.1	0.51	5.89	149.33 (118)
32	74.1	0.53	5.67	78.00
33	74.1	0.50	5.92	54.59
34	74.1	0.50	5.92	36.75

Note: Figures in parentheses show the time at which the interruption occurred.

M = 74.1 kgm (bending). In this graph the abscissas give the time and the ordinates show the displacement of the end plate δ in axial compression and the angle of rotation of the end plate α in bending. The moment of acceleration prior to failure apparently corresponds to the moment at which the first dent appeared. The change of relative ovalness during the bending test was about 0.1–0.2%.

A total of 38 shells was tested in axial compression, while a further 34 shells were tested in bending. The shells tested under a compressive load on TsDM-30 machines were made from the same batch of material (first batch), while the shells tested in bending and compression on lever-type machines were made from another batch of material (second batch). All the results are given in Tables 1 and 2.

During the compression tests loss of stability was accompanied by the formation of six to nine half-waves along the circumference and two to three rows of half-waves along the axis of the specimen. The shells that lost stability had exactly the same external appearance as shells after instantaneous loss of stability. In the bending tests waves were formed in the compression zone. In shape and size the waves were similar to the waves formed in axial compression.

For a quantitative evaluation the creep characteristics of the material were plotted for constant stress at 255 deg C. At each stress level 5–12 specimens made from tubes of each batch were tested on DST-5 and ZST 3/3 machines. The working length of these specimens was 100 mm and the diameter 8 mm. The average creep curves obtained by processing all the experimental data are given in Fig. 2 (the broken line represents the first batch and the solid line the second batch). According to [1] extruded tubes from D16T have at 250 deg C an elastic modulus of 5900 kg/mm², a shear modulus of 2080 kg/mm², and a proportionality limit of about 12 kg/mm².

Assuming for shells at 255 deg C a modulus of elasticity E = 5850 kg/mm² and Poisson's ratio $\mu = 0.42$, we obtain from the equations of [2] for shells without initial irregularities the maximum value of the critical compressive stress

$$\sigma^* = \frac{1}{\sqrt{3(1-\mu^2)}} E\frac{h}{R} = 0.64E\frac{h}{R} = 21.4 \text{ kg/mm}^2.$$

For the same shells with fairly large initial irregularities we use the lower value of the critical compressive stress

$$\sigma^{**} \simeq \frac{0.173}{\sqrt{(1-\mu^2)}} E\frac{h}{R} = 0.192E\frac{h}{R} = 6.2 \text{ kg/mm}^2.$$

Table 1 shows that instantaneous loss of stability of shells subjected to compressive stress takes place above the lower critical stress, thus indicating that the quality of shell manufacture was high. Loss of stability in creep takes place at loads above as well as below the lower critical stress. The wide scatter of the results is due to the fact that the shells all had different initial irregularities and the creep characteristics themselves show a considerable scatter.

Using the creep curves of Fig. 2 and the data of Table 1, we now estimate the total deformation of the middle surface at which the shell loses stability in creep. The ordinates of Fig. 3 represent the dimensionless stress $\sigma^\circ = \sigma/\sigma^*$, while the abscissas give the dimensionless total strain $\varepsilon^\circ = E\varepsilon/\sigma^*$, in which the instantaneous strain is assumed elastic, while the creep strain is determined from the creep curves of Fig. 2. Figure 3 shows that the total deformation at which loss of stability takes place in creep is smaller than the elastic strain corresponding to the upper critical stress, but larger than the elastic strain corresponding to the lower critical stress. The scatter of the experimental data increases with decreasing stress, i.e., with increasing creep strain. Exactly the same conclusion concerning the magnitude of the critical creep strain under compressive load in creep was obtained theoretically in [3] on the basis of nonlinear shell equations where the creep of the material was based on the aging hypothesis.

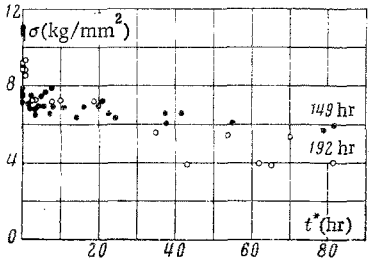

Fig. 4

A comparison of the experimental results on bending and axial compression of shells made from the second batch of material is given in Fig. 4. Here the abscissas are the critical time t^* and the ordinates are the average stress in axial compression or the maximum compressive stress at the initial moment in the case of bending.

Figure 4 shows that in the region of low stress levels the lowest values of the critical time are obtained for axial compression. Thus, the estimate of the critical time of loss of stability for shells in creep obtained from the elastic strain corresponding to the lower critical compressive stress σ^{**} gives a guaranteed lower value of the critical time both for compression and for bending.

REFERENCES

1. Manual of Aircraft Materials [in Russian], Oborongiz, vol. 2, 1958.

2. A. S. Vol'mir, Stability of Elastic Systems [in Russian], Fizmatgiz, 1963.

3. A. P. Kuznetsov and L. M. Kurshin, "On the calculation of the stability of shells in creep on the basis of the theory of aging," in: Problems of Stability in Building Mechanics [in Russian], Izd. liter. po stroitel'stvu, Moscow, 1965.

17 November 1964 Novosibirsk